

# Porous Versus Novel Compact Ziegler–Natta Catalyst Particles and Their Fragmentation During the Early Stages of Bulk Propylene Polymerization

Torvald Vestberg,<sup>1</sup> Peter Denifl,<sup>1</sup> Carl-Eric Wilén<sup>2</sup>

<sup>1</sup>Borealis Polymers Oy, P.O. Box 330, FIN-06101 Porvoo, Finland

<sup>2</sup>Functional Materials Center of Excellence, Laboratory of Polymer Technology, Åbo Akademi University, Biskopsgatan 8, FIN-20500 Åbo, Finland

Received 26 September 2007; accepted 26 February 2008

DOI 10.1002/app.28411

Published online 7 August 2008 in Wiley InterScience (www.interscience.wiley.com).

**ABSTRACT:** The effect of the porosity of Ziegler–Natta catalyst particles on early fragmentation, nascent polymer morphology, and activity were studied. The bulk polymerization of propylene was carried out with three different heterogeneous Ziegler–Natta catalysts under industrial conditions at low temperatures, that is, with a novel self-supported catalyst (A), a SiO<sub>2</sub>-supported catalyst (B), and a MgCl<sub>2</sub>-supported catalyst (C), with triethyl aluminum as a cocatalyst and dicyclopentyl dimethoxy silane as an external donor. The compact catalyst A exhibited no measurable porosity and a very low surface area (<5 m<sup>2</sup>/g) by Brunauer–Emmet–Teller analysis, whereas catalysts B and C showed surface areas of 63 and 250 m<sup>2</sup>/g, respectively. The surface and cross-sectional morphologies of the resulting polymer particles at different stages of particle growth were analyzed by scanning electron microscopy and transmission electron microscopy. The compact catalyst A showed homogeneous and instantaneous fragmen-

tation already in the very early stages of polymerization, which is typically observed for porous MgCl<sub>2</sub>-supported Ziegler–Natta catalysts. Moreover, the compact catalyst particles gave rise to almost perfectly spherical polymer particles with a smooth surface. In contrast, the silica-supported catalyst B gave rise to particles having a cauliflower morphology, and the second reference catalyst C produced fairly spherical polymer particles with a rough surface. All of the three catalysts exhibited similar activities of 450 g of polypropylene/g of catalyst after 30 min of polymerization, and most interestingly, the comparative kinetic data presented indicated that the reaction rates were not influenced by the porosity of the catalyst. © 2008 Wiley Periodicals, Inc. *J Appl Polym Sci* 110: 2021–2029, 2008

**Key words:** catalysts; electron microscopy; morphology; polyolefins; Ziegler–Natta polymerization

## INTRODUCTION

It is well known that the nature of a catalyst support plays an important role in the polymerization of olefins with Ziegler–Natta and single-site catalysts. According to most of this literature, the physical strength and porosity of the support and final catalyst have a strong influence on both the activity and polymer particle morphology. It was suggested early that it is the stress of the growing polymer that causes a progressive fragmentation of the catalyst particle.<sup>1</sup> Galli and coworkers<sup>2,3</sup> stressed that a catalyst used in propylene polymerization should have a high surface area and porosity and suitable mechanical strength to give high activity and good polymer powder morphology in an industrial process. It is also well recognized that fragmentation of the cata-

lyst during the early stage of polymerization is decisive for the final polymer powder morphology.

It is known that the MgCl<sub>2</sub>/TiCl<sub>4</sub> catalyst grain (macroparticle) is made up of many crystallites or primary catalyst particles, which likely agglomerate to form larger clusters (subparticles).<sup>4,5</sup> Cecchin and coworkers<sup>4,6</sup> suggested that the major contribution to catalyst porosity is the macropores formed by the interstitial spaces between subparticles. Ferrero et al.<sup>7</sup> concluded that the subparticles are accessible through the void space between growing catalyst/particle grains, which may facilitate monomer transport to the active sites.

Most of the work dealing with TiCl<sub>3</sub> and with MgCl<sub>2</sub>-supported TiCl<sub>4</sub> catalysts has shown that the initial fragmentation of these catalysts in propylene polymerization is normally uniform.<sup>5,7–11</sup> The polymerization starts everywhere in the catalyst particle more or less simultaneously, and in the early stage of polymerization, the catalyst is fragmented into individual primary catalyst particles, which are uniformly distributed in the polymer particle. Kaguko and coworkers<sup>9,10</sup> showed that the size of

Correspondence to: T. Vestberg (torvald.vestberg@borealisgroup.com).

Contract grant sponsor: Borealis Polymers Oy.

TABLE I  
Polymerization in Liquid Propylene at Low Temperatures

Polymerization time	Catalyst amount (mg)	Al/Ti (mol/mol)	TEA (mg)	Al/Do (mol/mol)	Hydrogen (mmol)	Temperature (°C)
6, 20, and 60 s	~ 50	5	11–24 <sup>a</sup>	10	2.3	30
3, 10, and 30 min	~ 17	15	11–24 <sup>a</sup>	10	2.3	20, 30, 40

Propylene (45 g) was used in a 125-mL reactor.

<sup>a</sup> The amount of TEA depended on the Ti content in the catalyst: 11, 20, and 24 mg were used for catalysts C, B, and A, respectively.

the catalyst fragments, when  $\text{TiCl}_3$  is used as a catalyst, is on the order of 10–20 nm, whereas the primary catalyst fragments in the case of  $\text{MgCl}_2$ -supported  $\text{TiCl}_4$  catalysts are on the order of 10–40 nm.<sup>5</sup>

$\text{MgCl}_2$ -supported  $\text{TiCl}_4$  catalysts do not always break up uniformly. Recently, Zheng and coworkers<sup>12–15</sup> showed that a  $\text{MgCl}_2$ -supported  $\text{TiCl}_4$  catalyst with a low surface area and porosity and small average pore size breaks up layer by layer. In contrast, a catalyst with a high surface area and porosity and average pore size gives what they called an *instantaneous breakup* under similar polymerization conditions.

Most of the studies related to fragmentation of the catalyst have been done under mild conditions. It is reasonable to believe that the rate of polymerization during fragmentation is also important to how the catalyst breaks up. Pater et al.<sup>16</sup> found that the initial reaction rate is the key factor in the determination of the final powder morphology. If the initial reaction rate is too high, regardless if this is because of a high polymerization temperature or a high hydrogen concentration, the morphology will be poor, which will cause a low bulk density.

In several studies in which  $\text{SiO}_2$  has been used as support, it has been observed that the initial fragmentation of this support normally proceeds layer by layer. This has been shown with a Ziegler–Natta catalyst for polyethylene<sup>17</sup> and with single-site catalysts for polypropylene (PP)<sup>18–20</sup> and polyethylene.<sup>21,22</sup> The strength and dimensions of the interconnecting network, in addition to the total pore volume, are important factors in the control of fragmentation and nascent polymerization with silica-based catalysts.<sup>23–26</sup>

More recently, there have been reports in the literature of a catalyst that has neither a measurable surface area nor porosity by Brunauer–Emmet–Teller (BET) analysis but still has a high activity and good powder morphology.<sup>27–34</sup> The catalyst gives roughly the same activity in the early stage of polymerization as a porous catalyst with the same chemistry under mild conditions. The catalyst gives good powder morphology under conditions used in industrial processes. The behavior of this catalyst seems to conflict with what we know is a prerequisite of good

catalysts: a high surface area and porosity. The target of this study was to investigate fragmentation of the catalyst when polymerization was conducted under typical industrial process conditions and to try to determine why the catalyst works so well despite its compactness.

## EXPERIMENTAL

### Materials

Propylene was obtained from a PP plant (Borealis, Finland) after purification and was further dried with molecular sieves before use in polymerization. Pentane was dried with molecular sieves and purged with nitrogen. Triethyl aluminum (TEA) was obtained from Chemtura Europe Ltd. (UK) and was used as received. Dicyclopentyl dimethoxy silane was obtained from Wacker (Germany) and was dried with molecular sieves and purged with nitrogen before use. Hydrogen (AGA) was of 99.999% purity.

### Preparation of the catalysts

Catalyst A was prepared in accordance with a novel emulsion-based catalyst preparation technology developed by Borealis Polymers Oy, as described elsewhere.<sup>33</sup> The catalyst was  $\text{MgCl}_2$ -supported. However, the support was not added as an external separately prepared support but was prepared *in situ* during catalyst preparation. Catalysts prepared according to this emulsion technology have no measurable pore volume and a very low surface area ( $<5 \text{ m}^2$ ) as measured with a Tristar 3000 BET instrument from Micromeritics. Catalyst B was prepared by Borealis Polymers Oy and is an example of a catalyst with silica as a support. This catalyst was based on the same emulsion system as catalyst A, but the preparation of the catalyst included as an additional step the addition of silica to the emulsion before solidification. Because of this, catalyst B had the same chemistry as catalyst A but was otherwise a typical silica-supported catalyst. Catalyst C can be described as a conventional fourth-generation Ziegler–Natta catalyst, with a high surface area and pore volume. This catalyst was used as an example

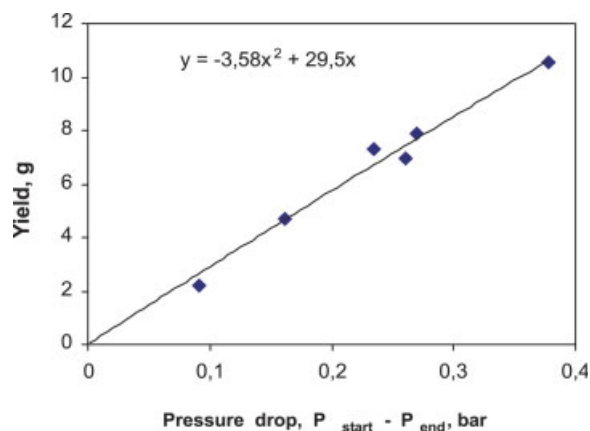


**Figure 1** Calibration curve describing the yield versus the pressure drop in the reactor when polymerization was conducted at 30°C. [Color figure can be viewed in the online issue, which is available at [www.interscience.wiley.com](http://www.interscience.wiley.com).]

of a catalyst that is known to give good polymer powder morphology in an industrial processes and must, consequently, have a controlled and homogeneous fragmentation.

### Polymerization procedure

The polymerizations were carried out in a 125-mL laboratory minireactor with TEA as the cocatalyst and dicyclopentyl dimethoxy silane as the external donor. The reactor was loaded with the different components (catalyst, cocatalyst, external donor, and 2.5 mL of pentane) in the glovebox and then connected to the rest of the reactor system. The contact time between the catalyst, cocatalyst, and external donor was 10 min. Finally, 2.3 mmol of hydrogen and 45 g of propylene were added. This amount of propylene in a reactor of this size meant that most of the monomer stayed in liquid form, and the polymerization was, thus, done in liquid propylene. The polymerization times were varied from 6 s up to

30 min. The polymerization was quenched by the addition of an excess of CO, and the yield was determined gravimetrically. The polymerization conditions are described in Table I. A high catalyst amount was used in the short-time polymerizations ( $\leq 1$  min) to enable accurate determination of the yield with gravimetric means. A low catalyst amount was used in the long-time polymerizations ( $\geq 3$  min) to prevent too-high conversion. The conversion was in all tests less than 20%. Instead of using the same Al/Ti ratio, we used the same TEA concentration, for a specific catalyst, in the short-time and long-time polymerizations.

The reactor contained 3 wt % pentane when the polymerization started. As the polymerization proceeded and propylene was consumed, the amount of pentane relative to the amount of propylene increased. This caused a pressure drop in the reactor, whereby the pressure measurements could be used to monitor the increase in yield over time. The calibration curve for translating the pressure drop into the amount of polymer produced is shown in Figure 1.

### Characterization of the polymer particles

Scanning electron microscopy (SEM) was used to follow catalyst fragmentation and to characterize the powder morphology. The equipment was a Quanta 200F from FEI Co. with high resolution and field emission. The catalyst and polymer particles were gold-coated before analysis at a high vacuum. The catalyst/polymer particles were embedded in epoxy resin and cut at room temperature. The cross-sectional pictures were taken without a gold coating and with a low vacuum.

Catalyst fragmentation was analyzed with transmission electron microscopy (TEM). The catalyst/polymer particles were embedded in epofix (Struers). Ruthenium tetroxid was used to harden and stain the sample. Sections 75–85 nm thick were cut on a Leica Ultracut E ultramicrotome with a diamond

**TABLE II**  
Characteristics of Catalysts A, B, and C

Catalyst	External support <sup>a</sup>	Ti (wt %)	BET area (m <sup>2</sup> /g) <sup>b</sup>	Pore volume (mL/g)	Average pore size (Å)	Average particle size (μm)
A	None <sup>c</sup>	3.8	<5 <sup>d</sup>	nm	nm	22
B	Silica <sup>e</sup>	3.6	63	0.25	159	28
C	MgCl <sub>2</sub>	1.9	290	0.50	68	57

<sup>a</sup> External support added during catalyst synthesis.

<sup>b</sup> The porosity (surface area, pore volume, and average pore size) of the catalysts was measured with the BET method with nitrogen physisorption with a Tristar 3000 instrument.

<sup>c</sup> This catalyst contained no external separately prepared support but contained MgCl<sub>2</sub> prepared *in situ* during catalyst preparation.

<sup>d</sup> Below the detection limit of BET.

<sup>e</sup> In addition to silica as an external support, this catalyst contained MgCl<sub>2</sub> prepared *in situ* during catalyst preparation. The silica grade was ES 747 JR from Ineos.

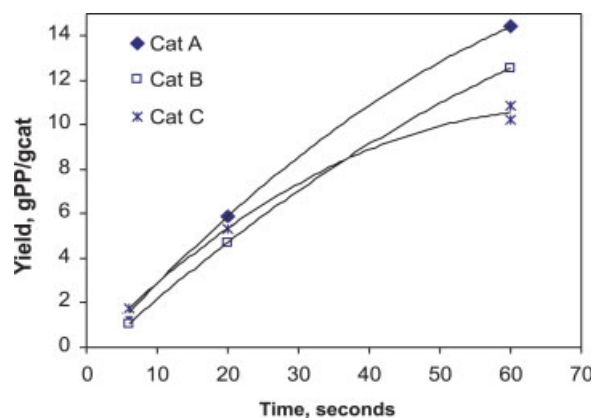


**Figure 2** Yield versus the time during the first tens of seconds of the polymerization of propylene at 30°C. The propylene conversion in the 60-s test was about 1.5%. [Color figure can be viewed in the online issue, which is available at [www.interscience.wiley.com](http://www.interscience.wiley.com).]

knife (Diatome). The images were taken with Tecnai G<sup>2</sup> 12 (FEI Co.) equipped with a charged coupling device camera (Gatan Bioscan) at 100 kV.

## RESULTS AND DISCUSSION

The catalyst characteristics of catalysts A, B, and C in terms of composition, porosity, pore volume, and average particle size are presented in Table II. We observed from the BET investigations with nitrogen physisorption that in contrast to catalysts B and C, catalyst A did not exhibit any measurable pore volume and exhibited a very small surface area. The lack of measurable porosity was attributed to the compact nature of the catalyst particles obtained with emulsion technology.

Propylene polymerizations were carried out in liquid propylene with the aforementioned Ziegler–Natta catalyst systems to investigate the influence of the porosity on catalyst fragmentation. Typical curves of yield versus polymerization time for short polymerization times for catalysts A, B, and C are depicted in Figure 2. The compact catalyst A started as fast as the porous reference catalyst and even faster than the porous silica-supported catalyst C. The compactness of catalyst A did not clearly negatively influence how the polymerization started and proceeded, at least not during this time frame of 6 s up to 1 min. The silica-supported catalyst produced only 1.1 g of PP/g of catalyst during the first 6 s of polymerization, whereas the other two catalysts produced 1.6–1.8 g of PP/g of catalyst. Later in polymerization, all three catalysts had roughly the same performance, so the silica-supported catalyst definitely had a slow start. This indicated that the fragmentation of this catalyst occurred more slowly than that of catalysts A and C. A less fragmented catalyst

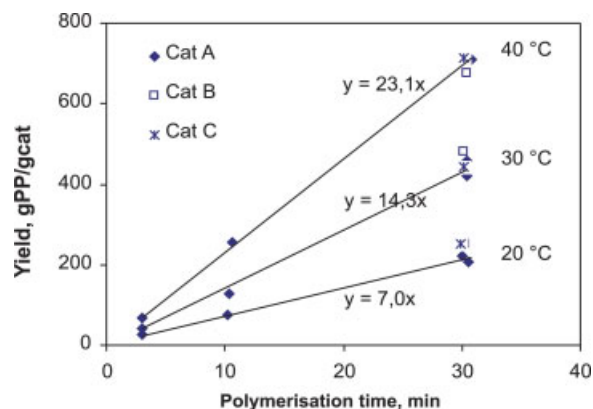


**Figure 3** Increase in the yield over time at different temperatures. The line for catalyst A was drawn with linear regression with 0 as the intercept. [Color figure can be viewed in the online issue, which is available at [www.interscience.wiley.com](http://www.interscience.wiley.com).]

means more restriction for the monomer to reach active sites, and as a consequence, the activity of the silica-based catalyst was lower in the very early stage of polymerization. This may be interpreted in the way that the silica-supported catalyst had an induction time, which has been reported in literature when silica with a low porosity was used in Ziegler–Natta-catalyzed propylene polymerization.<sup>13</sup> The results in Figure 2 show the overall activity for all particles in the test. It has been shown that silica-supported catalyst particles, similar to catalyst B in this study, have an uneven start.<sup>25</sup> Some of the catalyst particles do not start to grow immediately upon monomer exposure but only after a certain period of inhibition. This is probably the reason why the silica-supported catalyst in these tests had a slow start.

The activity decreased slightly with time during this time period for all three catalysts (Fig. 2). A similar decrease in activity during the first minutes of

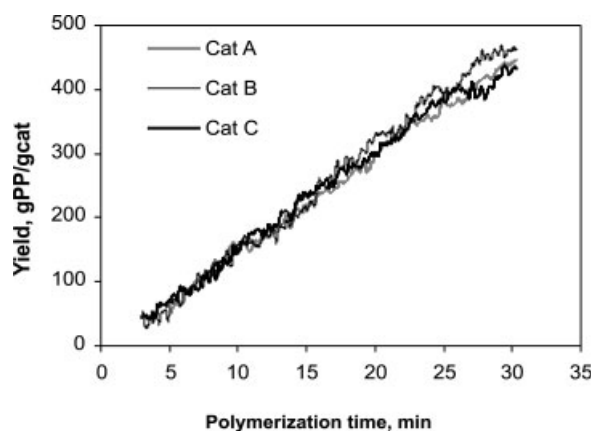


**Figure 4** Increase in the yield over time calculated from the pressure drop in the reactor for the polymerization at 30°C.

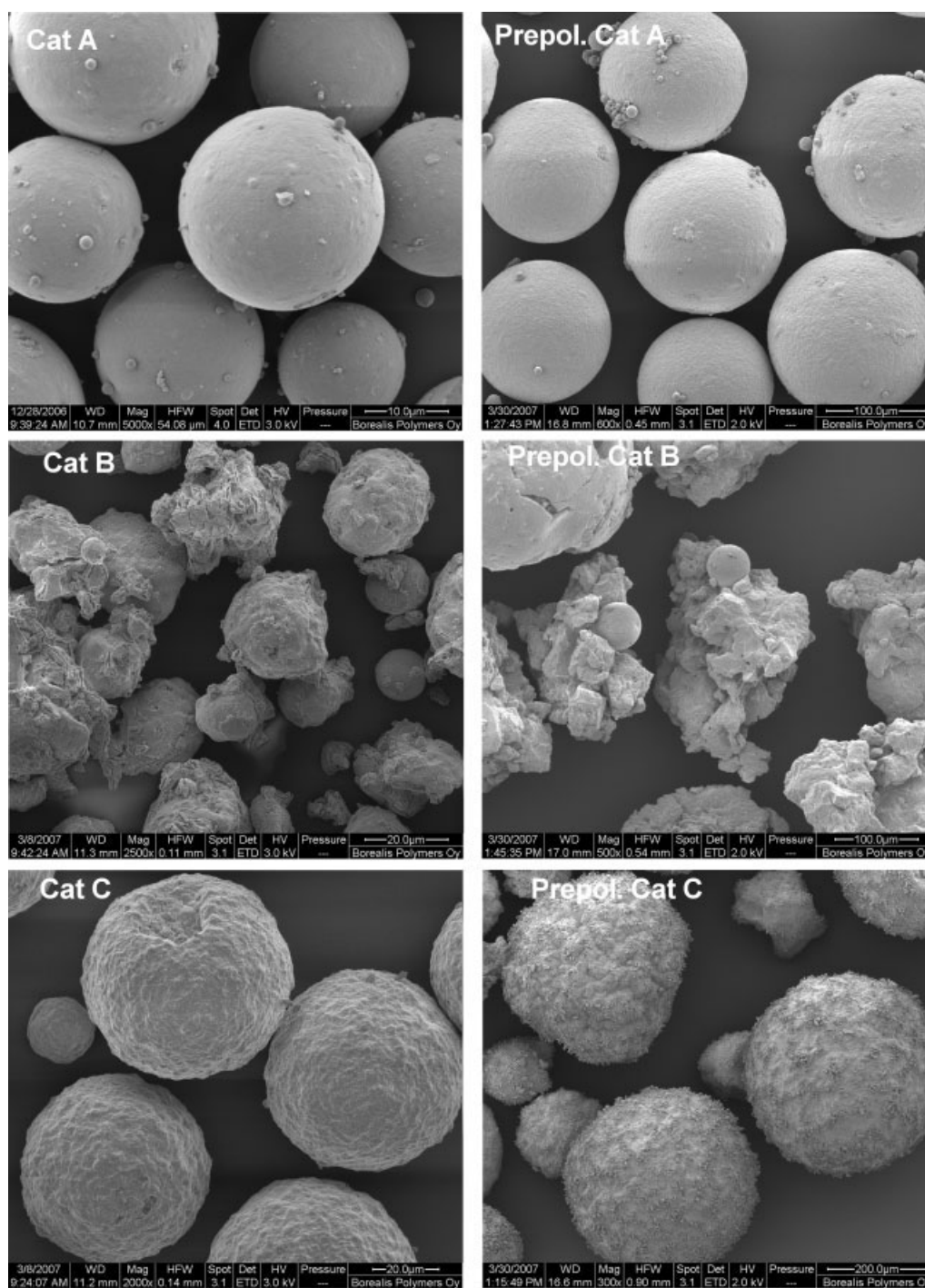


**Figure 5** SEM pictures of the morphology of the catalysts and the polymer particles (labeled Prepol. Cat in the figure). Polymerization was performed at 30°C, and the polymerization time was 30 min. The degree of polymerization was about 450 g of PP/g of catalyst for all three catalysts.

polymerization, under milder conditions than used here, was reported in the literature.<sup>14</sup> The decrease in activity was attributed to the encapsulating effect of the produced polymer around the active centers in the early stage of polymerization. The polymer-rich phase around the active center had a lower monomer concentration than the surrounding me-

dium. This explanation fit well with our findings. During the first tens of seconds, the activity decreased because of the encapsulating effect, but later on, during polymerization times of 3–30, when the catalyst was completely fragmented and the active centers were well covered by polymeric material, the activity reached a constant level, which was

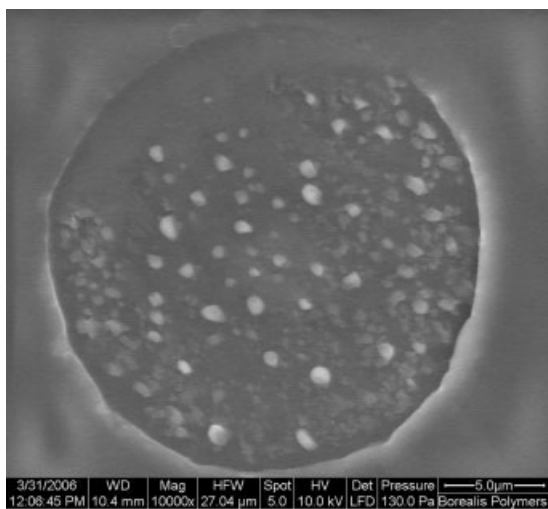


**Figure 6** Cross-sectional SEM picture of a catalyst/polymer particle after 6 s of polymerization at 30°C with catalyst A. The degree of polymerization was 1.6 g of PP/g of catalyst.

seen as a constant increase in yield (Figs. 3 and 4). The effect of increasing polymerization temperature on activity was similar for the three catalysts. The activity almost doubled for every 10°C between 20 and 40°C. This indicated that the compact catalyst A behaved in the same way as the porous catalysts with regard to activity.

Interestingly, the decrease in activity during the early stage of polymerization observed under dilute conditions reported in literature was also valid for the polymerization in liquid propylene under industrial conditions.

All three catalysts had a linear increase in yield, and the final yield was almost the same for all three of them (Fig. 4). A linear increase in yield over time

means that the rate of reaction was constant under these conditions over this time period of polymerization. This is perhaps not surprising when one considers that the highest yield in these tests corresponded only to less than 1% of what the catalysts were capable of producing and that the conversions in these tests were kept on a low level, on the order of 8–20%. It is clear from Figure 4 that during this time period of 3–30 min, the compact catalyst A performed as well as the porous catalysts. In the 30-min polymerizations, the silica-supported catalyst, which seemed to have a slightly slower start, performed as well as the other two catalysts, apparently because the catalyst was, at that point, completely fragmented.

As shown by the presented data, the compact catalyst had a fast start, and the rate of reaction in no way seemed to be restricted by the compactness of the catalyst.

### Morphology of the polymer particles

The polymer powders produced in the experiments were analyzed with SEM and TEM. All three catalysts exhibited the well-known replica phenomena; that is, the original shape of the catalyst particle was maintained during polymerization (Fig. 5). The compact catalyst A consisted of almost perfectly spherical particles with smooth surfaces. The polymer particle produced with catalyst A looked very similar to the original catalyst, only bigger. This indicated that the fragmentation process proceeded in a controlled and homogeneous way. The silica-supported catalyst B had an angular and uneven morphology, which did not change during polymerization. The particles also just became bigger. The porous reference

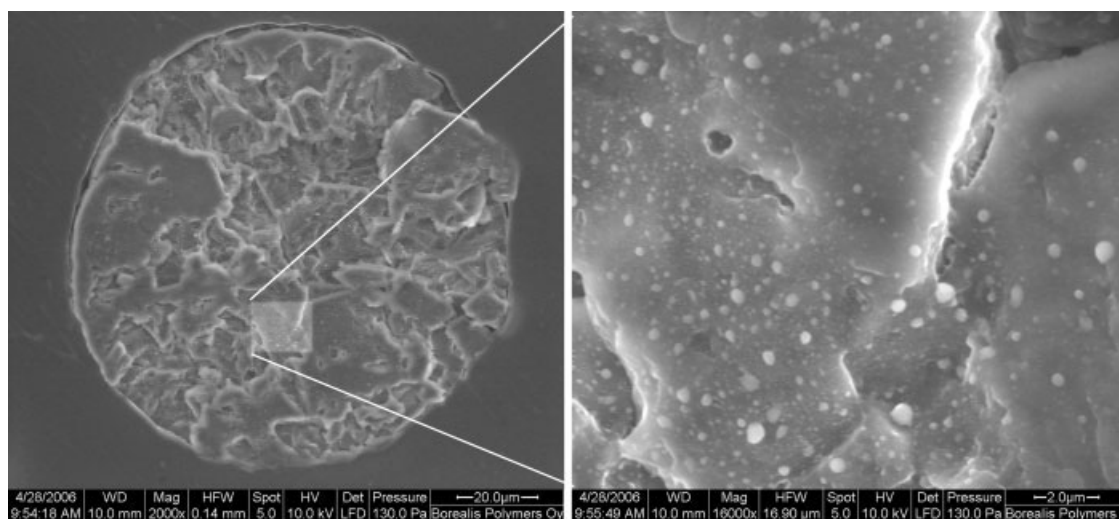


**Figure 7** Cross-sectional SEM picture of a catalyst/polymer particle after 6 s of polymerization at 30°C with catalyst C. The degree of polymerization was 1.8 g of PP/g of catalyst.

catalyst C had a rough surface, which was also seen in the polymer particle. The polymerization was done at 30°C for Figure 5. If polymerization was done at 20 or 40°C, the morphology was similar to that shown in Figure 5. The only difference was that polymerization at 20°C gave slightly smaller particles and polymerization at 40°C gave slightly bigger particles. This, in combination with the yield versus time data shown in Figure 3, indicated that all three catalysts, including compact catalyst A, broke up in a homogeneous and controlled way over the entire temperature range, 20–40°C, under these conditions.

One area where differences between compact catalyst A and the porous catalysts was anticipated was the way in which the catalyst fragmentation progressed during the first seconds of polymerization. One might expect that catalyst A should have broken up layer by layer, as has been shown in the literature with MgCl<sub>2</sub>-supported Ziegler–Natta catalysts with low porosities and surface areas.<sup>12,13</sup> However; this was not the case for the compact catalyst A particles. After 6 s of polymerization, corresponding to 1.6 g of PP/g of catalyst, the catalyst had started to break up and the fragmentation had started uniformly everywhere in the particle (Fig. 6). At this stage, the particles consisted of small catalyst fragments embedded in a polymer-rich phase. The size of the biggest catalyst fragments was on the order of 0.8 μm. After 20 s of polymerization, corresponding to 6 g of PP/g of catalyst, the catalyst fragments were so small that they were no longer visible with this technique.

The porous reference catalyst C broke up in the same way as catalyst A. After 6 s of polymerization, the fragmentation had started everywhere, and the size of the biggest catalyst fragments was about 0.6 μm (Fig. 7). After 20 s of polymerization, the fragments were no longer visible.

It has been shown in the literature that conventional MgCl<sub>2</sub>-supported Ziegler–Natta catalysts normally break up uniformly under mild conditions; the fragmentation starts everywhere more or less simultaneously. In this study, a conventional porous catalyst, also under industrial conditions in liquid propylene, broke up uniformly. Also, the fragmentation of compact catalyst A in liquid propylene was uniform. This showed that catalyst A behaved like conventional porous catalysts, despite its compactness.

From TEM pictures of the catalyst/polymer particles after 1 min of polymerization, corresponding to 10–14 g of PP/g of catalyst, the fragmentation process had proceeded so far that the catalyst fragments had come down to a size that in the literature is normally ascribed to the size of the primary catalyst particles (Fig. 8). The size and the rodlike shape of the catalyst fragments with catalyst A indicated

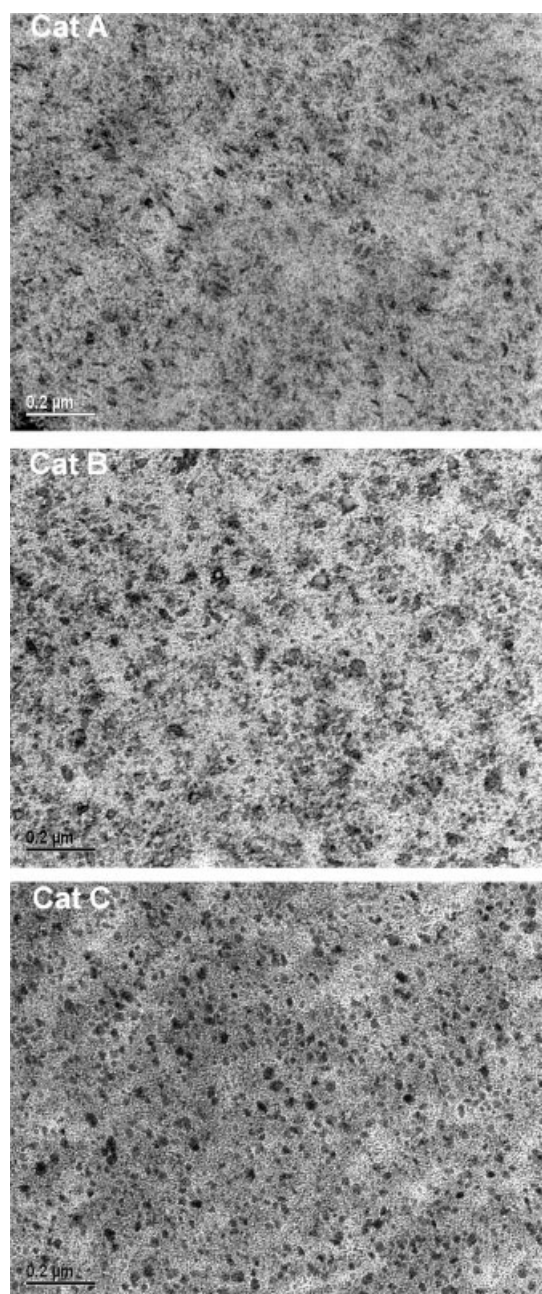


**Figure 8** TEM pictures of the particles after 1 min of polymerization at 30°C. The degree of polymerization was 10–14 g of PP/g of catalyst.

that the fragments were the primary catalyst particles. The length of the fragments was on the order of 35–40 nm. These catalyst fragments were clearly seen also when the porous reference catalyst C was used. With this catalyst, the size of the fragments seemed to be more spherical and perhaps slightly bigger than when with catalyst A. The picture of the silica-based catalyst B was more complicated, probably because of the presence of both MgCl<sub>2</sub> fragments and silica fragments. The bigger fragments, about 60 nm, were probably silica fragments.

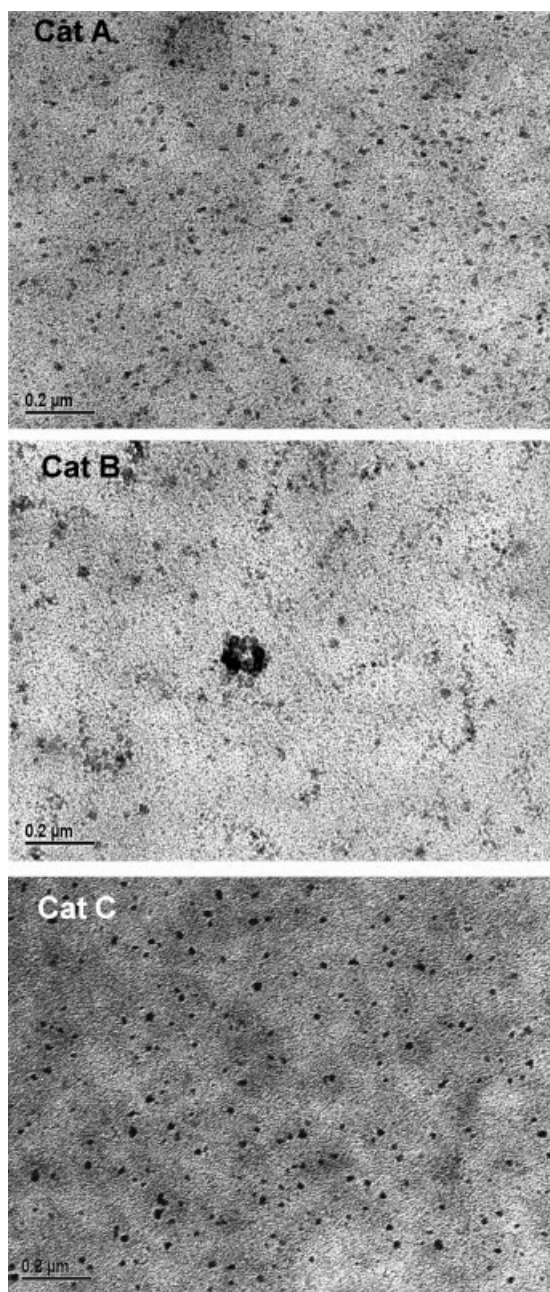


**Figure 9** TEM pictures of the particles after 30 min of polymerization at 30°C. The degree of polymerization was about 450 g of PP/g of catalyst.

The overall picture did not change so much with the 30-min polymerization, except that the catalyst fragments were more separated (Fig. 9). For compact catalyst A and porous reference catalyst C, the size of the catalyst fragments did not change between 1 and 30 min of polymerization. This showed that the catalyst was already fragmented down to the size of the primary catalyst particles after 1 min of polymerization under these conditions. This was evidence that the fragmentation process progressed as

fast with compact catalyst A as with porous reference catalyst C. The polymerized silica-supported catalyst B had some small dark dots, which presumably were  $\text{MgCl}_2$  fragments. It also contained quite a lot of 0.1–0.2  $\mu\text{m}$  sized fragments, which were probably silica fragments.

## CONCLUSIONS

The importance of the catalyst support has been demonstrated many times in prior literature. It has been postulated that to have good activity and good morphology in propylene polymerization, the catalyst must be porous and have a high surface area. Compact catalyst A had no measurable porosity and a very low surface area as determined by BET analysis, and still, the catalyst possessed good activity and morphology. The catalyst also exhibited homogeneous fragmentation in the early stages of propylene polymerization, as is typically observed for porous  $\text{MgCl}_2$ -supported Ziegler–Natta catalysts. In summary, we concluded that even compact catalyst particles may undergo instant and uniform fragmentation at the beginning of polymerization under industrial conditions and, in this respect, behave in the same manner as highly porous Ziegler–Natta catalyst particles.

The authors gratefully acknowledge Borealis Polymers Oy for its approval to publish this research. Elisabeth Ingolic (Center for Electron Microscopy, Technical University, Graz, Austria) is gratefully acknowledged for making the transmission electron microscopy images. Ismo Lehtiniemi and Vuokko Ojanperä are acknowledged for running the polymerizations and for making the scanning electron microscopy pictures, respectively.

## References

1. Natta, G.; Pasquon, I. *Adv Catal* 1959, 11, 1.
2. Galli, P.; Luciani, L.; Cecchin, G. *Angew Makromol Chem* 1981, 94, 63.
3. Galli, P.; Barbè, P. C.; Noristi, L. *Angew Makromol Chem* 1984, 120, 73.
4. Cecchin, G.; Marchetti, E.; Baruzzi, G. *Macromol Chem Phys* 2001, 202, 1987.
5. Noristi, L.; Marchetti, E.; Baruzzi, G.; Sgarzi, P. *J Polym Sci Part A: Polym Chem* 1994, 32, 3047.
6. Cecchin, G.; Morini, G.; Pelliconi, A. *Macromol Symp* 2001, 173, 195.
7. Ferrero, M. A.; Koffi, E.; Sommer, R.; Conner, W. C. *J Polym Sci Part A: Polym Chem* 1992, 30, 2131.
8. Ferrero, M. A.; Sommer, R.; Spanne, P.; Jones, K. W.; Conner, W. C. *J Polym Sci Part A: Polym Chem* 1993, 31, 2507.
9. Kakugo, M.; Sadatoshi, H.; Yokoyama, M.; Kojima, K. *Macromolecules* 1989, 22, 547.
10. Kakugo, M.; Sadatoshi, H.; Sakai, J.; Yokoyama, M. *Macromolecules* 1989, 22, 3172.
11. Pater, J. T. M.; Weickert, G.; Loos, J.; van Swaaij, W. P. M. *Chem Eng Sci* 2001, 56, 4107.



12. Zheng, X.; Pimplapure, M. S.; Weickert, G.; Loos, J. *Macromol Rapid Commun* 2006, 27, 15.
13. Zheng, X.; Loos, J. *Macromol Symp* 2006, 236, 249.
14. Pimplapure, M. S.; Zheng, X.; Loos, J.; Weickert, G. *Macromol Rapid Commun* 2005, 26, 1155.
15. Zheng, X.; Pimplapure, M. S.; Weickert, G.; Loos, J. *e-Polymers* 2006, No. 028.
16. Pater, J. M. T.; Weickert, G.; van Swaaij, W. P. M. *J Appl Polym Sci* 2003, 87, 1421.
17. Niegisch, W. D.; Crisafulli, S. T.; Nagel, T. S.; Wagner, B. E. *Macromolecules* 1992, 25, 3910.
18. Zheng, X.; Smit, M.; Chadwick, J. C.; Loos, J. *Macromolecules* 2005, 38, 4673.
19. Knoke, S.; Korber, F.; Fink, G.; Tesche, B. *Macromol Chem Phys* 2003, 204, 607.
20. Fink, G.; Tesche, B.; Korber, F.; Knoke, S. *Macromol Symp* 2001, 173, 77.
21. Smit, M.; Zheng, X.; Brüll, R.; Loos, J.; Chadwick, J. C.; Koning, C. E. *J Polym Sci Part A: Polym Chem* 2006, 44, 2883.
22. Smit, M.; Zheng, X.; Loos, J.; Chadwick, J. C.; Koning, C. E. *J Polym Sci Part A: Polym Chem* 2006, 44, 6652.
23. Weist, E. L.; Ali, A. H.; Naik, B. G.; Conner, W. C. *Macromolecules* 1989, 22, 3244.
24. Webb, S. W.; Conner, W. C.; Laurence, R. L. *Macromolecules* 1989, 22, 2885.
25. Tait, P. J. T.; Moman, A. A. *Kinet Catal* 2006, 47, 2, 284.
26. McDaniel, M. P. *J Polym Sci Polym Chem Ed* 1981, 19, 1967.
27. Pöhler, H.; Denifl, P.; Leinonen, T.; Vestberg, T. Presented at MetCon, Houston, TX, 2003.
28. Denifl, P.; Leinonen, T. Presented at EUPOC, Milan, Italy, 2003.
29. Leinonen, T.; Denifl, P.; Vestberg, T. Presented at EUPOC, Milan, Italy, 2003.
30. Vestberg, T.; Denifl, P.; Leinonen, T. Presented at Nordic Polymer Days, Åbo, Finland, 2004.
31. Bartke, M.; Oksman, M.; Mustonen, M.; Denifl, P. *Macromol Mater Eng* 2005, 290, 250.
32. Abboud, M.; Denifl, P.; Reichert, K.-H. *Macromol Mater Eng* 2005, 290, 558.
33. Abboud, M.; Denifl, P.; Reichert, K.-H. *J Appl Polym Sci* 2005, 98, 2191.
34. Abboud, M.; Denifl, P.; Reichert, K.-H. *Macromol Mater Eng* 2005, 290, 1220.